

# Non-LTE, Relativistic Accretion Disk Fits to 3C 273 and the Origin of the Lyman Limit Spectral Break

Omer Blaes

Department of Physics, University of California, Santa Barbara, CA 93106

Ivan Hubeny

AURA/NOAO, NASA Goddard Space Flight Center, Code 681, Greenbelt, MD 20771

Eric Agol<sup>1</sup>

Theoretical Astrophysics, MS 130-33, California Institute of Technology, Pasadena, CA 91125

and

Julian H. Krolik

Department of Physics and Astronomy, Johns Hopkins University, Baltimore, MD 21218

## ABSTRACT

We fit general relativistic, geometrically thin accretion disk models with non-LTE atmospheres to near simultaneous multiwavelength data of 3C 273, extending from the optical to the far ultraviolet. Our model fits show no flux discontinuity associated with a hydrogen Lyman edge, but they do exhibit a spectral break which qualitatively resembles that seen in the data. This break arises from relativistic smearing of Lyman emission edges which are produced locally at tens of gravitational radii in the disk. We discuss the possible effects of metal line blanketing on the model spectra, as well as the substantial Comptonization required to explain the observed soft X-ray excess. Our best fit accretion disk model underpredicts the near ultraviolet emission in this source, and also has an optical spectrum which is too red. We discuss some of the remaining physical uncertainties, and suggest in particular that an extension of our models to the slim disk regime and/or including nonzero magnetic torques across the innermost stable circular orbit may help resolve these discrepancies.

*Subject headings:* accretion, accretion disks — galaxies: active — quasars: individual (3C 273)

---

<sup>1</sup>Chandra fellow

## 1. Introduction

Accretion disks around supermassive black holes are widely believed to be the source of the optical/ultraviolet continuum in many classes of active galactic nuclei (AGN). The reasons for this include the expectation that gravitational potential energy is efficiently converted into radiation in disks and the prediction that the emergent spectrum peaks in the optical or ultraviolet. In addition, a disk provides a possible site for producing the X-ray reflection features observed in Seyferts (Nandra & Pounds 1994), including a relativistically broadened iron  $K\alpha$  line (Tanaka et al. 1995).

The agreement between accretion disk model predictions and observations of optical/ultraviolet radiation from AGN is far from satisfactory, however (see e.g. Koratkar & Blaes 1999, Krolik 1999a, and Collin 2001 for recent reviews). Among the oft-cited problems is the absence of observed flux discontinuities at the Lyman limit of hydrogen (Antonucci, Kinney, & Ford 1989; Koratkar, Kinney, & Bohlin 1992), in contrast to the large absorption edges which were predicted to exist in early theoretical investigations of accretion disk atmospheres (Kolykhalov & Sunyaev 1984). However, a number of effects can weaken these predicted edges. Rather high photospheric densities in the early models were in part responsible for the large absorption edges (Czerny & Pojmański 1990). Later investigations showed that for sufficiently high accretion rates, lower photospheric densities were produced, which reduced the edges or even drove them into emission in individual atmosphere models (Coleman 1993, Shields & Coleman 1994, Hubeny & Hubeny 1997, Sincell & Krolik 1997). Non-LTE effects also reduce discontinuities at the Lyman limit (Sun & Malkan 1989; Shields & Coleman 1994; Störzer, Hauschildt, & Allard 1994; Hubeny & Hubeny 1997). Comptonization by a hot corona can smear out Lyman edges (Czerny & Zbyszewska 1991; Lee, Kriss, & Davidsen 1992; Hsu & Blaes 1998). Finally, many authors have shown that relativistic Doppler effects and gravitational redshifts can smear out an edge in the integrated spectrum of a disk (Sun & Malkan 1989, Laor & Netzer 1989, Laor 1992, Lee et al. 1992, Coleman 1993, Shields & Coleman 1994, Wehrse 1997).

A small fraction of objects ( $\sim 10$  percent of those investigated; Koratkar 1998; Koratkar & Blaes 1999) exhibit “partial Lyman edges” in which there is no sharp flux discontinuity, but there is a change in continuum slope near  $912 \text{ \AA}$ . Examples include the type 1 Seyfert Mrk 335 (Zheng et al. 1995) and the QSO PG 1630+377 (Koratkar et al. 1995). A spectral break near the Lyman limit is also observed in the *Hubble Space Telescope*/FOS composite quasar spectrum (Zheng et al. 1997).

Recently, Kriss et al. (1999, hereafter KDZL) have presented *Hopkins Ultraviolet Telescope* (*HUT*) data for 3C 273 which also appear to show a spectral break near the Lyman limit. More precisely, they observed the source at two epochs (December 1990 and

March 1995), and found that single power-laws failed to provide adequate fits to the far ultraviolet continuum in both epochs. Broken power-laws, with breaks at  $\sim 900 \text{ \AA}$  in the quasar rest frame, provided better fits, although the improvement was substantial for the first epoch only.

Appenzeller et al. (1998) have also presented far ultraviolet data on this quasar taken with the *ORFEUS-II* mission. Their raw, reddened spectrum shows no obvious features near the intrinsic Lyman limit of the quasar, but they did not present any actual fits to the continuum. They noted that for their observations to be consistent with longer wavelength *International Ultraviolet Explorer (IUE)* data, a turnover near an observed wavelength of  $1200 \text{ \AA}$  ( $\simeq 1040 \text{ \AA}$  in the quasar rest frame) was required. This is the longest wavelength in the *ORFEUS-II* data, and the *IUE* comparison data was not simultaneous, so the reality of this turnover is uncertain.

3C 273 was the first AGN to have its optical continuum compared to accretion disk models (Shields 1978). KDZL also applied crude accretion disk models and found a reasonable fit at both epochs. Their models consisted of a multitemperature blackbody disk orbiting a Schwarzschild black hole, with an ad hoc absorption edge at the Lyman limit, together with a spherical Comptonizing corona of unit Thomson depth. The temperature of the corona was constrained so as to fit the soft X-ray spectrum which was observed simultaneously with *BBXRT* and nearly simultaneously with *ROSAT* during the December 1990 *HUT* observations. This epoch also had nearly simultaneous optical (KPNO) and *IUE* data. While doing a good job in the ultraviolet and the X-rays, KDZL acknowledged that their fits had a number of problems. First, they failed to produce a break as sharp as that observed near the Lyman limit, i.e. their model overpredicted the far ultraviolet. In addition, it underpredicted the optical portion of the spectrum. In order to fit the far ultraviolet break as well as they could, their models all had high disk inclinations of  $\sim 60^\circ$ . As they noted, the disk is more likely to be nearly face-on given that the source has a superluminal jet. Finally, their best fit model to the December 1990 data had an Eddington ratio of 0.46, violating their assumption of a geometrically thin disk.

We have recently computed an extensive grid of non-LTE accretion disk models for a wide range of black hole masses and accretion rates, in both Schwarzschild and Kerr spacetimes (Hubeny et al. 2000, hereafter HABK). In agreement with earlier studies, flux discontinuities at the Lyman limit are generally not present for high luminosity disks. Moreover, we find that breaks in the continuum slope near the Lyman limit are common. A superluminal source like 3C 273 provides a stringent test of the Lyman edge problem because relativistic smearing is smallest in a face-on disk. We have fit nearly face-on models to the 3C 273 data and find a qualitatively reasonable fit to the observed spectral

break, with no flux discontinuity, even with no Comptonization. We therefore propose that spectral breaks near the Lyman limit in quasars may simply be due to relativistic smearing of edges produced at different radii in the accretion disk.

This paper is organized as follows. In § 2 we describe the model fits to the data. Our model fits are far from perfect, and in § 3 we explore some of the physical effects that we have not included which could affect the spectra in the vicinity of the Lyman limit. Then in § 4 we discuss the implications of these fits and compare them to work by previous authors. We also discuss how the broadband fits might be improved by extending our models into the regime of slim disks, or by including magnetic torques across the innermost stable circular orbit. We summarize our conclusions in § 5.

## 2. Accretion Disk Model Fits

### 2.1. *HUT* Data

The observations and analysis of the December 1990 *BBXRT*, *HUT*, *IUE*, and KPNO data are described in detail in KDZL. We first concentrate on model fits to the *HUT* data, which contain the Lyman edge region. We will discuss later the broadband spectrum at both shorter and longer wavelengths.

The HABK grid of Kerr ( $a/M = 0.998$ ) models covers nine black hole masses from  $1/8 \times 10^9$  to  $32 \times 10^9 M_{\odot}$ , each value a factor of two larger than the next smaller mass. For each mass, eleven models were computed with accretion rates a power of two times one solar mass per year, again spaced by factors of two. The highest accretion rate for each mass was chosen to make the overall luminosity approximately 0.3 times the Eddington limit. Spectra were computed using our relativistic transfer function (Agol 1997) for an observer at infinity viewing the disk at a discrete set of inclination angles  $i$  given by  $\cos i = 0.01, 0.2, 0.4, 0.5, 0.6, 0.8, \text{ and } 0.99$ . The only remaining quantity is the viscosity parameter  $\alpha$ . HABK considered two values, 0.01 and 0.1, but found that this made little difference to the resulting spectra except at very high frequencies in the He II Lyman continuum. As this lies in the unobserved gap between the far ultraviolet and soft X-rays in 3C 273, we consider only the  $\alpha = 0.01$  models in this paper.

In our fitting process, we first transform our models from the quasar rest frame to the observer frame. We adopt a redshift of 0.158 for 3C 273, a Hubble constant  $H_0 = 70 \text{ km s}^{-1} \text{ Mpc}^{-1}$ , and a spatially flat cosmology with  $\Omega_M = 1/3$  and  $\Omega_{\Lambda} = 2/3$ . We then accounted for Galactic extinction by reddening our model spectrum. We considered values of  $E(B - V)$  ranging from 0.02 (as determined from the *DIRBE* dust infrared

emission map of Schlegel, Finkbeiner, & Davis 1998) to 0.032 (as determined from the HI column density measurements of Lockman and Savage 1995).<sup>2</sup> Assuming  $R_V = 3.1$ , we then reddened our models using the Cardelli, Clayton, & Mathis (1989) extinction curve. Unfortunately, the hydrogen Lyman limit of 3C 273 lies at  $1056\text{\AA}$ , where the extinction curve is somewhat uncertain. We comment on this further in section 4 below.

At this point, we interpolated our model spectra onto the observed *HUT* data wavelengths and then added quasar emission and Galactic absorption lines to our models according to the broken power law continuum fits presented in tables 4 and 6 of KDZL. Following KDZL, we also accounted for the fifty lowest energy Galactic hydrogen Lyman absorption lines as well as the Lyman continuum, assuming a neutral hydrogen column density of  $1.8 \times 10^{20} \text{ cm}^{-2}$ , and Voigt profiles with Doppler parameters of  $15 \text{ km s}^{-1}$  convolved with the Gaussian instrument resolution profile of  $3\text{\AA}$  FWHM.

Finally, we measured  $\chi^2$  by comparing our model with the observed *HUT* data. We excluded the observed wavelength regions  $980\text{-}1000\text{\AA}$ ,  $1194\text{-}1238\text{\AA}$ ,  $1287\text{-}1319\text{\AA}$ , and  $1820\text{-}1870\text{\AA}$  from our fits because of contamination by terrestrial airglow lines. We also excluded all observed wavelengths shortward of  $915\text{\AA}$  because these wavelengths are affected by the highest order Lyman lines, which we did not model.

We performed this procedure for our entire grid of non-LTE models, searching for the model with the mass  $M$ , accretion rate  $\dot{M}$ , and inclination  $i$  which had the lowest  $\chi^2$ . Note that these fits were made with the absolute spectral flux density, i.e. we fit both the shape and normalization of the spectrum. The best fit models turned out to be  $M = 1.6 \times 10^{10} M_\odot$ ,  $\dot{M} = 4 M_\odot \text{ yr}^{-1}$ , and  $\cos i = 0.4$  and  $0.5$  for  $E(B - V) = 0.02$  and  $0.032$ , respectively, with corresponding values of  $\chi^2 = 2522$  and  $2866$  for 1577 data points. However, a number of models turned out to have comparable values of  $\chi^2$ . Due perhaps to the coarse graining of accretion rates in our grid (successive values being separated by factors of two), almost all these models had accretion rates of  $4 M_\odot \text{ yr}^{-1}$ . This was independent of the Galactic extinction, and is clearly driven by the normalization of the spectrum.

Figure 1 illustrates how one of these models compares to the *HUT* data. While the fit appears quite reasonable at long wavelengths, it does not do a good job at the shortest wavelengths and in fact is still not adequate given the value of  $\chi^2$ . Part of the reason for

---

<sup>2</sup>Our treatment differs slightly from KDZL, who assumed a cosmology with zero deceleration parameter and  $H_0 = 75 \text{ km s}^{-1} \text{ Mpc}^{-1}$ . Our rest frame flux densities are therefore 23 percent higher than theirs. In addition, KDZL adopted a Galactic  $E(B - V)$  of 0.032 in their paper, although their figures 6-8 in fact used  $E(B - V) = 0.02$  (G. Kriss 2000, private communication).

the high value of  $\chi^2$  may be because we did not try refitting the lines with our continuum models. As these lines are not the focus of this paper, we instead use this particular fit to isolate six continuum windows at quasar rest wavelengths of 826-830, 864-872, 955-959, 1093-1099, 1354-1360, and 1445-1455Å.<sup>3</sup> We performed a weighted average of the data in these six regions, and then repeated our entire fitting procedure, this time neglecting lines entirely, and now letting the reddening float between 0.2 and 0.032. The best fit model was the same:  $M = 1.6 \times 10^{10} M_{\odot}$ ,  $\dot{M} = 4 M_{\odot} \text{ yr}^{-1}$ , and  $\cos i = 0.4$  with  $\chi^2 = 12$  for  $E(B - V) = 0.024$ . Given that we have only six data points, this is not a good fit statistically. Figure 2 shows the reason: this particular model is unable to reproduce the curvature in the turnover at the shortest wavelengths.

3C 273 is a superluminal source, so models with such high inclinations are physically ruled out. The observed VLBI proper motions give apparent transverse velocities ranging from 7.0 to 11  $c$  for our Hubble constant (e.g. Abraham et al. 1996). The larger value directly implies  $\cos i > 0.98$ . However, the apparent velocities of the superluminal components which originated near 1990, the year of the multiwavelength campaign data considered here, were closer to the smaller value, giving  $\cos i > 0.96$ . Abraham & Romero (1999) have developed a kinematic precession model of the 3C 273 jet which gives  $\cos i \simeq 0.98$  for the December 1990 epoch.

Again fitting to just the continuum points, the best fit nearly face-on model ( $\cos i = 0.99$ ) was  $M = 2 \times 10^9 M_{\odot}$ ,  $\dot{M} = 4 M_{\odot} \text{ yr}^{-1}$  and  $E(B - V) = 0.0253$ , giving  $\chi^2 = 76$ . Figure 3 illustrates this model fit. The model clearly does a better job at reproducing the short wavelength slope (and therefore the overall spectral break) than the more edge-on model shown in figure 2, but it also exhibits a bump that peaks redward of the quasar rest-frame Lyman limit. The origin of these features can be seen in figure 4, which shows a crude estimate of the contributions that individual annuli make to the far ultraviolet region of the spectrum. We multiplied the local rest-frame emergent spectral flux from each annulus by an “area” computed in a Newtonian fashion from the Boyer-Lindquist coordinate radius and width (figure 4a), and then added this power to that from other annuli in the model (figure 4b). This provides a quick illustration of what determines the total spectrum, but we stress that our full model properly takes into account the general relativistic proper area of each emitting element, as well as gravitational redshifts, Doppler shifts, and bending of photon trajectories to the observer. Figure 4 shows clearly that in the absence of these relativistic effects, the disk would produce a Lyman edge in emission.

---

<sup>3</sup>Recent high resolution *Far Ultraviolet Spectroscopic Explorer* spectra of 3C 273 by Sembach et al. (2001) cover the first three wavelength regions and confirm that they are devoid of large equivalent width absorption lines.

This edge is completely smeared out, however, in models with significant inclination with respect to the observer, such as in figure 2. Gravitational redshifts and the transverse Doppler effect also smear and redden this edge in the nearly face-on model shown in figure 3, producing a bump redward of the rest-frame Lyman limit. We stress that even in this case, there is no flux discontinuity, although there is a marked change in spectral slope.

HABK also computed a grid of models around Schwarzschild holes, and these gave similar results. The best fit non-LTE model to the continuum data points was  $M = 4 \times 10^9 M_\odot$ ,  $\dot{M} = 22 M_\odot \text{ yr}^{-1}$ ,  $\cos i = 0.5$ , and  $E(B - V) = 0.032$ , with  $\chi^2 = 23$ . This model has the same overall luminosity as the best fit Kerr models. The best nearly face-on Schwarzschild model had  $M = 10^9 M_\odot$ ,  $\dot{M} = 11 M_\odot \text{ yr}^{-1}$ , and  $E(B - V) = 0.032$ , with  $\chi^2 = 389$ . The Schwarzschild models are clearly much worse than the Kerr models, suggesting that some black hole spin may be required in this source. This may confirm theoretical ideas that jet production is related to black hole spin, but we caution the reader not to draw strong conclusions given the poor quality of our fits.

## 2.2. Optical/Ultraviolet Multiwavelength Data

The December 1990 observing campaign also had near simultaneous *IUE* and optical (KPNO) data. The accretion disk is putatively responsible for much of this emission as well, so we also tried fitting this data. In terms of rest wavelengths, we identified 1795-1805Å as a continuum window in the *IUE*/LWP data, and 4190-4210, 4700-4720, 5090-5110, and 5590-5610Å as continuum windows in the optical KPNO data. Based on the emission line studies of I Zw 1 by Boroson & Green (1992) and Laor et al. (1997), these windows avoid most of the potential Fe II line blends. Unfortunately, we did not have access to the error bars on this data, so we estimated the variance by calculating it directly using an unweighted average of the data points in each wave band. Combined with the six *HUT* continuum points, we therefore had eleven points in total in our continuum dataset.

3C 273 is known to exhibit correlated variability between the optical and infrared (Cutri et al. 1985), suggesting some contamination of the big blue bump by emission from the jet. However, the median optical polarization is less than 0.5 percent (Impey, Malkan & Tapia 1989), and the polarized flux can be fit with a steep power law  $F_\nu \propto \nu^{-1.9}$  (Wills 1989). Jet contamination is therefore negligible throughout the far ultraviolet *HUT* data, but it might be an important contributor in the optical. We therefore considered models with an additional  $F_\nu \propto \nu^{-1.9}$  power law, normalized to be ten percent of the observed

optical (5500 Å) emission (Impey et al. 1989).<sup>4</sup>

The best fit non-LTE, nearly face-on ( $\cos i = 0.99$ ) Kerr disk model to the multiwavelength data was the same as that for the *HUT* data alone:  $M = 2 \times 10^9 M_\odot$  and  $\dot{M} = 4 M_\odot \text{ yr}^{-1}$ . The best fit extinction was  $E(B - V) = 0.0261$  with the blazar component ( $\chi^2 = 187$ ) and  $E(B - V) = 0.024$  without the blazar component ( $\chi^2 = 126$ ). Figures 5 and 6 illustrate these model fits to the data.

The slope of the optical continuum data is substantially bluer than our disk model, a fact which is true for all the models we present in this paper. Fitting a power law through the four optical data points gives a spectrum  $F_\lambda \propto \lambda^{-2.43 \pm 0.12}$ , or  $F_\nu \propto \nu^{0.43 \pm 0.12}$ . While this is bluer than most bright quasars (e.g. Francis et al. 1991), we note that the reddened optical/near infrared data presented in Lichti et al. (1995) for this source are also comparably blue. Even if we applied no reddening and no red blazar component to our best fit disk model, it would only have an optical spectrum as blue as  $F_\nu \propto \nu^0$ . It could be that our optical continuum points suffer from contamination by emission lines. Figure 6 shows clear evidence for broad line emission at the shortest optical wavelengths, though as stated above we tried to avoid this in our choice of continuum points.

### 3. Modifications to the Basic Disk Models

The HABK models leave out some potentially important physics. Here we consider two additional effects which may alter the spectrum of 3C 273 around the Lyman limit of hydrogen.

#### 3.1. Metal Line Blanketing

The HABK models completely neglect line opacities from all atomic species. Numerous ultraviolet lines of various metal species exist in hot atmospheres, and this may significantly affect the emergent spectrum of a disk in the Lyman limit region (Hubeny & Hubeny 1998).

To gauge how important this is, we have recomputed the emergent spectrum through our best fit Kerr disk model ( $M = 2 \times 10^9 M_\odot$  and  $\dot{M} = 4 M_\odot \text{ yr}^{-1}$ ), including line opacities from the thirty lightest elements (H-Zn). We did this by recomputing the radiative transfer

---

<sup>4</sup>Our fits to the *HUT* data alone which we discussed previously also included this miniblazar component. Because it is so small in the far ultraviolet, the best fit models do not change, but the actual values of  $\chi^2$  which we quoted do depend slightly on this.

in our converged atmosphere model for each annulus with line opacities included, but we did not recompute the atmosphere model. The line opacities and source functions were taken to be in LTE, with thermal Doppler line profiles. The resulting spectra do not conserve flux because energy balance with the additional opacities is not enforced. The normalization of the spectrum is therefore not to be trusted, but spectral features associated with the opacity sources may survive a self-consistent treatment. In any case, these spectra provide an indication of the importance of metal line blanketing.

Figure 7 shows the resulting far ultraviolet spectrum, compared to that without line blanketing. The parameters are exactly the same as those of our best fit model shown in Figure 3. The qualitative features of the model spectrum remain the same: there is still no flux discontinuity at the Lyman limit, and there is still a spectral break. However, line blanketing appears to *enhance* the residual bump left over from smearing the Lyman emission edges of individual annuli, by absorbing flux both longward and shortward of the edge. Whether this will be preserved in more self consistent modeling which maintains flux conservation and includes non-LTE effects remains to be seen.

### 3.2. Comptonization and the Soft X-ray Excess of 3C 273

We have recently computed a series of disk models which include the effects of Comptonization within the disk structure itself, assuming that the energy dissipation rate per unit mass is vertically constant within each annulus (Hubeny et al. 2001). For the black hole masses and accretion rates we have found to be relevant for 3C 273, these Comptonized models differ negligibly in the optical-ultraviolet region from the models computed by HABK which we have used here.

The December 1990 observing campaign also included *BBXRT* and *ROSAT* observations, which together show the presence of a clear soft X-ray excess. Such emission is not present in any of our models (including the Comptonized models of Hubeny et al. 2001). A possible explanation for the soft excess is the presence of an additional, much stronger, Comptonizing component (e.g. KDZL). Such a component might change the observed shape of the far ultraviolet continuum.

In order to investigate this, we followed KDZL and Comptonized our disk spectra using the crude prescription of Czerny & Zbyszewska (1991). We treated the disk spectrum (already folded through the relativistic transfer function) as a point source in a spherical cloud of hot electrons described by two parameters: an electron temperature and a radial Thomson depth. It is likely that the hot electrons are closer to the disk, and a better

physical treatment would be to locally Comptonize the spectra of each of our annuli, but our simple-minded treatment should still be sufficient to capture the main qualitative effects.

We defined soft X-ray fluxes by averaging the *ROSAT* data, corrected for interstellar absorption, in quasar rest frame wavelength ranges of 30-40 and 40-50Å. We found an acceptable fit to these fluxes by Comptonizing our  $M = 2 \times 10^9 M_{\odot}$ ,  $\dot{M} = 4 M_{\odot} \text{ yr}^{-1}$ ,  $\cos i = 0.99$ , Kerr model with a cloud of unit radial Thomson depth and temperature  $3.3 \times 10^8 \text{ K}$ . A reddening of  $E(B - V) = 0.032$  then provided the best fit to the optical/ultraviolet data. Comparisons between the Comptonized models and the data are shown in figures 8 and 9.

This Comptonized model provided an improved (though still unacceptable) fit to the *HUT* data alone, giving  $\chi^2 \simeq 50$ . Figure 9 shows why: Comptonization has smeared out the small Lyman edge bump feature in the spectrum. The overall quality of the fit to the optical and ultraviolet data remained about the same, however, because Comptonization has little effect at longer wavelengths.

#### 4. Discussion

Quantitatively, all our model fits to the continuum data are rather poor. There are numerous reasons why this might be so, as we will discuss later in this section. However, we still believe that our fits represent a qualitative success, as there is no sign of a Lyman edge flux discontinuity. This is true even though we are using face-on models, which minimize the effects of relativistic Doppler smearing of the intrinsic Lyman edges formed locally at each radius of the disk. All that remains of the Lyman edge is a small bump shifted redward from the Lyman limit. As we showed in section 3, this bump itself may well be modified by the effects of line opacities and the Comptonization necessary to produce the observed soft X-ray excess. Although there is no Lyman edge, there is a spectral break in the vicinity of the Lyman limit, in qualitative agreement with that seen in the data. In addition, while our models do a poor job of explaining the slope of the optical data, they are much better here than the model fits of KDZL which substantially underpredicted the optical flux (cf. Fig. 7 of their paper).

Compared to the (Schwarzschild) fits of KDZL, our black hole mass is 2-3 times larger and our accretion rate is 3 times smaller. Our best fit model has a luminosity  $\simeq 0.3$  times the Eddington limit, i.e. is marginally consistent with the disk being geometrically thin. (This best-fit model is in fact at the edge of our grid of models for this reason.) Previous

authors have obtained roughly similar values for the black hole mass and accretion rate when trying to fit the overall shape of the big blue bump with much simpler accretion disk models. For example, Shields (1978) found  $M = 10^9 M_\odot$  and  $\dot{M} = 3 M_\odot \text{ yr}^{-1}$  for a Newtonian multitemperature blackbody disk with an underlying power law component extended from the infrared. Ramos et al. (1997) fit optical/ultraviolet data taken in 1994 and 1995 with multitemperature modified blackbody disk models around a maximal Kerr hole and found  $M = 10^9 M_\odot$  and an accretion rate  $\dot{M} = 2.4 M_\odot \text{ yr}^{-1}$ . Due to the high radiative efficiency of accretion onto a Kerr hole, this corresponds to a luminosity  $\simeq 0.5$  the Eddington limit, too high for the disk to be truly geometrically thin.

Our accretion disk models also have rather large absorption edges near the hydrogen Balmer limit. As noted by HABK, these edges are not to be trusted as they arise from cool annuli in the disk which have vertical density inversions and steep, convectively unstable temperature profiles, at least within our treatment of the vertical disk structure. Direct comparison of this region of the spectrum with the data is difficult due to contamination by the “little blue bump”, thought to be caused by Balmer continuum and FeII line emission from the broad line region (BLR) of the quasar.

The annuli responsible for the emission near the Lyman limit are also convectively unstable due to our assumed vertical dissipation profile and the fact that they are supported by radiation pressure (Agol et al. 2001, see also the discussion of Hubeny et al. 2001). How this might affect the Lyman edge locally at each annulus is unclear, and we are currently pursuing models that incorporate vertical convective transport of heat, as well as investigating different vertical profiles of the energy dissipation rate (e.g. Miller & Stone 2000). However, radiation pressure may have even more serious effects on the structure of the disk. Turbulence in a radiation dominated environment may result in strong density contrasts, invalidating our approximation of a smooth density profile which depends only on height within the annulus (Begelman 2001; Turner, Stone, & Sano 2001). Thermal and viscous instabilities may also exist which might give rise to an inhomogeneous disk structure (Krolik 1998), as well as invalidating the assumption of a stationary flow. Unfortunately, we cannot as yet predict how these effects might change the results of our spectral computations.

Our current models also neglect reprocessing of external radiation, including that due to bending of light rays from other parts of the disk. This could be important at far ultraviolet wavelengths, particularly in the near-maximal Kerr models we showed here (Cunningham 1976).

We remind the reader that we tried fitting models corresponding to only two black hole spins:  $a/M = 0$  and  $0.998$ . It could be that intermediate black hole spins might produce

improved fits. To investigate this, we tried fitting near face-on, multitemperature blackbody models to the data using a range of accretion rates, black hole masses, and spins. Figure 10 illustrates such a model, corresponding to  $a/M = 0.7$ . This model produces a much better fit to the far ultraviolet data ( $\chi^2 \simeq 8$ ) than our best fit near face-on disk model made from stellar atmospheres, although it is still a statistically poor fit. We stress that it contains little physics! The smooth turnover at short wavelengths in the model spectrum is largely produced by the Galactic reddening. The fact that the far ultraviolet fit is still poor suggests that a sharper spectral break than can be produced by reddening alone is required. Moreover, this model still fails to produce an optical spectrum as blue as that observed. We computed a hydrogen/helium disk model with stellar atmospheres along the lines of the HABK models, with the same parameters as this multitemperature blackbody model, and found a much worse fit than our nearly maximal Kerr models. We therefore believe that models with intermediate black hole spins will not solve the remaining qualitative discrepancies in our spectral fits.

A recent measurement of Galactic far ultraviolet extinction by Sasseen et al. (2001) finds that the wavelength dependence is slightly flatter in shape than the extrapolation of the Cardelli et al. (1989) curve we have used throughout this paper. This provides increased confidence that the observed spectral break is in fact intrinsic to the quasar. However, it is clearly desirable to try fitting a miniblazar like 3C 273 which is at somewhat higher redshift so that one could be certain that any spectral break observed near the Lyman limit is less affected by the shape of the extinction curve.

#### 4.1. Could the Accretion Flow in 3C 273 be a Slim Disk?

Our models do a good job of explaining the lack of a Lyman edge in this quasar, and in producing a far ultraviolet spectral break comparable to what is observed. However, they are far from producing a statistically acceptable fit. The chief discrepancies are a redder optical spectrum than is observed, and an underprediction of the  $\lambda_{\text{obs}} = 1500 - 2000\text{\AA}$  ultraviolet emission. In order to resolve these discrepancies, one must alter the radial effective temperature profile of the optically emitting annuli to be closer to the asymptotic  $r^{-3/4}$  law. This will then produce a bluer optical spectrum (as blue as  $F_\nu \propto \nu^{1/3}$ ), and would also therefore help enhance the  $1500 - 2000\text{\AA}$  ultraviolet emission. At the same time, one must ensure that the overall luminosity of the annuli responsible for the far ultraviolet emission remains approximately the same, in order to continue to fit the observed spectrum in the region of the Lyman limit.

It is noteworthy that our best fit model is already at the maximum Eddington

ratio  $L/L_{\text{Edd}} = 0.3$  consistent with a geometrically thin disk. Increasing the Eddington ratio still further, either by lowering the black hole mass or by increasing the accretion rate, would push the optically emitting annuli further out in radius, where the  $r^{-3/4}$  effective temperature profile holds. It would also move the disk into the regime of slim disks (Szuszkiewicz, Malkan & Abramowicz 1996). Slim disks differ from standard thin disks primarily in the role played by advection. This flattens the inner radial profile of effective temperature, thereby reducing the far ultraviolet emission compared to what would be expected if the flow was describable as a thin disk. It also produces more extreme ultraviolet/soft X-ray emission, an effect which will be enhanced by Comptonization within the flow.

Another effect which could alter the models in the same direction is a nonzero torque on the disk at the innermost stable circular orbit. Such a torque might be exerted through magnetic fields anchored in the flow (Krolik 1999b, Gammie 1999). Its primary effect is to enhance the radiative efficiency, which could be compensated for by reducing the accretion rate. At the same time, reprocessing of the relatively enhanced inner disk radiation at larger radii would cause the effective temperature profile to approach  $r^{-3/4}$  at smaller radii (Agol & Krolik 2000), which would produce an optical spectrum that is more blue.

It is possible that these effects will provide a much improved fit to the 3C 273 data. We therefore intend to extend our detailed atmosphere modeling to the slim disk regime in future, as well as investigate nonzero inner torques. We stress again that most quasars have optical colors which are much redder than those of 3C 273, and therefore more in agreement with the HABK disk models. A parameter which distinguishes 3C 273 from other quasars, such as a high Eddington ratio, is therefore an attractive possibility for explaining its unusually blue optical spectrum.

## 5. Conclusions

We have fit near face-on, bare accretion disk models to the multiwavelength data obtained by KDZL in the December 1990 observing campaign of 3C 273. These models fully account for non-LTE effects in hydrogen and helium in the disk atmospheres, and also include a full treatment of general relativistic effects in the disk structure as well as photon propagation to the observer. Our model fits are far from perfect, underpredicting the near ultraviolet emission and producing an optical spectrum which is too red. However, they produce no flux discontinuities near the Lyman limit. Instead, a small bump in the spectrum exists, which arises from gravitational redshifts and the transverse Doppler effect acting on individual Lyman emission edges emitted locally at tens of gravitational radii.

We performed a preliminary investigation of the effects of line blanketing, which appear to enhance this bump, while the Comptonization required to explain the observed soft X-ray excess smears it out. Our models produce a spectral break in the vicinity of the Lyman limit which is in qualitative agreement with observation.

There are a number of other problems with accretion disk models that we have not addressed in this paper. In particular, the near simultaneous variability observed throughout the optical/ultraviolet in AGN almost certainly requires that reprocessing contribute to the emission at some level, and we have not incorporated such reprocessing at all in our disk models. Moreover, some quasars with partial Lyman edges have dramatically increased polarization blueward of the Lyman limit (Impey et al. 1995, Koratkar et al. 1995), a problem which still has no satisfactory explanation within the accretion disk paradigm (see Shields, Agol, & Blaes 2000 for a recent review).

We nevertheless believe that the model fits shown here demonstrate substantially improved agreement between theory and observation of the Lyman limit region in quasars. For 3C 273 itself, the most important next step will be to extend our models into the slim disk regime, and possibly consider nonzero external torques across the innermost stable circular orbit. These effects should reduce the discrepancies between the model and the data in the near ultraviolet and optical portions of the spectrum.

We thank Gerard Kriss for generously making available to us the observational data used in this paper, Beverley Wills for discussions on possible nonthermal contamination of the big blue bump in 3C 273, and Tim Sasseen for discussions on far ultraviolet extinction. This work was supported by NASA grant NAG5-7075 and NSF grant PHY-9907949.

## REFERENCES

- Abraham, Z., Carrara, E. A., Zensus, J. A., & Unwin, S. C. 1996, *A&AS*, 115, 543
- Abraham, Z., & Romero, G. E. 1999, *A&A*, 344, 61
- Agol, E. 1997, Ph.D. thesis, Univ. California, Santa Barbara
- Agol, E., & Krolik, J. H. 2000, *ApJ*, 528, 161
- Agol, E., Krolik, J. H., Turner, N., & Stone, J. 2001, *ApJ*, in press
- Antonucci, R. R. J., Kinney, A. L., & Ford, H. C. 1989, *ApJ*, 342, 64

- Appenzeller, I., Krautter, J., Mandel, H., Bowyer, S., Dixon, W. V., Hurwitz, M., Barnstedt, J., Grewing, M., Kappelman, N., & Krämer, G. 1998, *ApJ*, 500, L9
- Begelman, M. C. 2001, *ApJ*, 551, 897
- Boroson, T. A., & Green, R. F. 1992, *ApJS*, 80, 109
- Cardelli, J. A., Clayton, G. C., & Mathis, J. S. 1989, *ApJ*, 345, 245
- Coleman, H. H. 1993, PhD Thesis, University of Texas, Austin, TX
- Collin, S. 2001, in *GH Advanced Lectures on the Starburst-AGN Connection*, eds. D. Kunth & I. Aretxaga, in press (astro-ph/0101203)
- Cunningham, C. 1976, *ApJ*, 208, 534
- Cutri, R. M., Wiśniewski, W. Z., Rieke, G. H., & Lebofsky, M. J. 1985, *ApJ*, 296, 423
- Czerny, B., & Pojmański, G. 1990, *MNRAS*, 245, 1P
- Czerny, B., & Zbyszewska, M. 1991, *MNRAS*, 249, 634
- Francis, P. J., Hewett, P. C., Foltz, C. B., Chaffee, F. H., Weymann, R. J., & Morris, S. L. 1991, *ApJ*, 373, 465
- Gammie, C. F. 1999, *ApJ*, 522, L57
- Hubeny, I., Agol, E., Blaes, O., & Krolik, J. H. 2000, *ApJ*, 533, 710 (HABK)
- Hubeny, I., Blaes, O., Krolik, J. H., & Agol, E. 2001, *ApJ*, in press
- Hubeny, I., & Hubeny, V. 1997, *ApJ*, 484, L37
- Hubeny, I., & Hubeny, V. 1998, in *Accretion Processes in Astrophysical Systems: Some Like it Hot!*, ed. S. S. Holt & T. R. Kallman (Woodbury, NY: AIP), 171
- Impey, C. D., Malkan, M. A., & Tapia, S. 1989, *ApJ*, 347, 96
- Impey, C., Malkan, M., Webb, W., & Petry, C. 1995, *ApJ*, 440, 80
- Kolykhalov, P. I., & Sunyaev, R. A. 1984, *Adv. Space Res.*, 3, 249
- Koratkar, A. 1998, in *Accretion Processes in Astrophysical Systems: Some Like it Hot!*, ed. S. S. Holt & T. R. Kallman (Woodbury, NY: AIP), 150

- Koratkar, A., Antonucci, R. R. J., Goodrich, R. W., Bushouse, H., & Kinney, A. L. 1995, *ApJ*, 450, 501
- Koratkar, A., & Blaes, O. 1999, *PASP*, 111, 1
- Koratkar, A. P., Kinney, A. L., & Bohlin, R. C. 1992, *ApJ*, 400, 435
- Kriss, G. A., Davidsen, A. F., Zheng, W., & Lee, G. 1999, *ApJ*, 527, 683 (KDZL)
- Krolik, J. H. 1998, *ApJ*, 498, L13
- Krolik, J. H. 1999a, *Active Galactic Nuclei* (Princeton: Princeton Univ. Press)
- Krolik, J. H. 1999b, *ApJ*, 515, L73
- Laor, A. 1992, in “Testing the AGN Paradigm”, ed. S. S. Holt, S. G. Neff, & C. M. Urry, 155
- Laor, A., Jannuzi, B. T., Green, R. F., & Boroson, T. A. 1997, *ApJ*, 489, 656
- Laor, A., & Netzer, H. 1989, *MNRAS*, 238, 897
- Lee, G., Kriss, G. A., & Davidsen, A. F. 1992, in “Testing the AGN Paradigm”, ed. S. S. Holt, S. G. Neff, & C. M. Urry, 159
- Lichti, G. G., et al. 1995, *A&A*, 298, 711
- Lockman, F. J., & Savage, B. D. 1995, *ApJS*, 97, 1
- Miller, K. A., & Stone, J. M. 2000, *ApJ*, 534, 398
- Nandra, K., & Pounds, K. A. 1994, *MNRAS*, 268, 405
- Ramos, E., Kafatos, M., Fruscione, A., Bruhweiler, F. C., McHardy, I. M., Hartman, R. C., Titarchuk, L. G., & von Montigny, C. 1997, *ApJ*, 482, 167
- Sasseen, T. P., Hurwitz, M., Dixon, W. V., & Airieau, S. 2001, *ApJ*, in press
- Sembach, K. R., Howk, J. C., Savage, B. D., Shull, J. M., & Oegerle, W. M. 2001, *ApJ*, in press
- Schlegel, D. J., Finkbeiner, D. P., & Davis, M. 1998, *ApJ*, 500, 525
- Shields, G. A. 1978, *Nature*, 272, 706

- Shields, G. A., Agol, E., & Blaes, O. 2000, in *The Seventh Texas-Mexico Conference on Astrophysics: Flows, Blows and Glows*, ed. W. Lee & S. Torres-Peimbert, in press
- Shields, G. A., & Coleman, H. H. 1994, in *Theory of Accretion Disks*, ed. W. J. Duschl et al. (NATO ASI Ser. C, 417; Dordrecht: Kluwer), 223
- Sincell, M. W., & Krolik, J. H. 1998, *ApJ*, 496, 737
- Störzer, H., Hauschildt, P. H., & Allard, F. 1994, *ApJ*, 437, L91
- Sun, W.-H., & Malkan, M. A. 1989, *ApJ*, 346, 68
- Szuskiewicz, E., Malkan, M. A., & Abramowicz, M. A. 1996, *ApJ*, 458, 474
- Tanaka, Y., et al. 1995, *Nature*, 375, 659
- Turner, N. J., Stone, J. M., & Sano, T. 2001, *ApJ*, submitted
- Wehrse, R. 1997, in “*Accretion Phenomena and Related Outflows*”, ed. D. T. Wickramasinghe, L. Ferrario, & G. V. Bicknell (San Francisco: ASP), 162
- Wills, B. J. 1989, in “*BL Lac Objects*”, ed. L. Maraschi, T. Maccacaro, & M.-H. Ulrich (Berlin: Springer), 109
- Zheng, W., et al. 1995, *ApJ*, 444, 632
- Zheng, W., Kriss, G. A., Telfer, R. C., Grimes, J. P., & Davidsen, A. F. 1997, *ApJ*, 475, 469

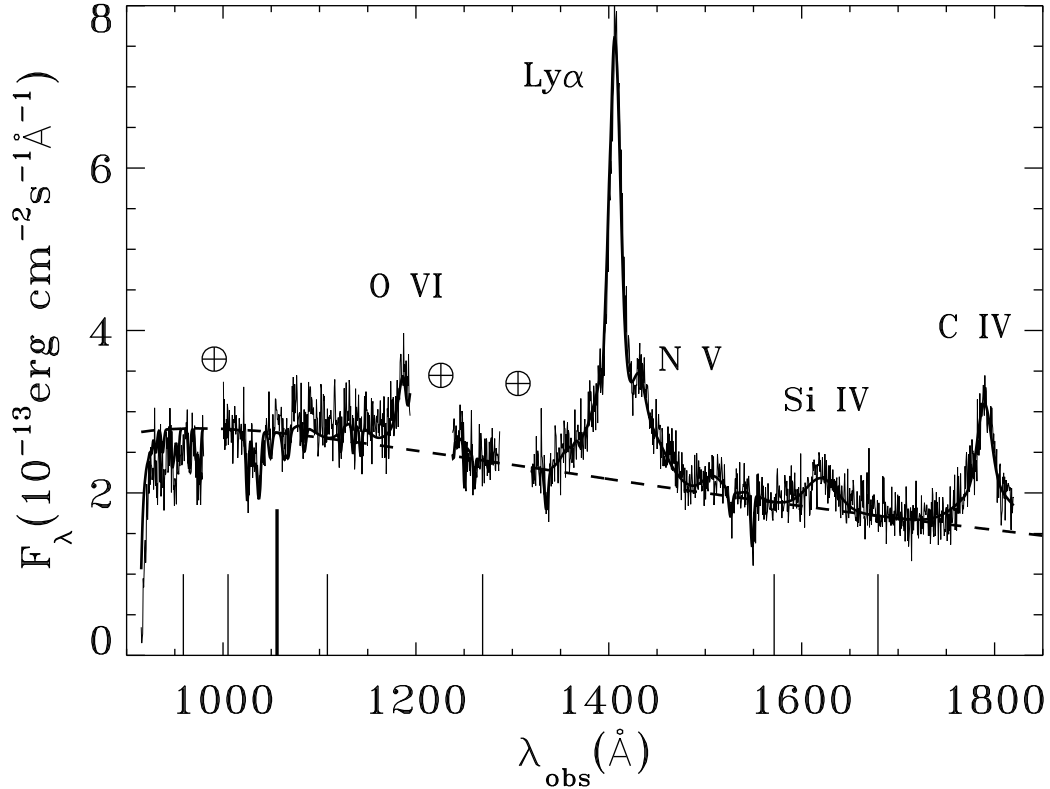


Fig. 1.— Best fit non-LTE Kerr disk continuum model to the December 1990 3C 273 *HUT* data (noisy curves), assuming a fixed reddening of  $E(B-V) = 0.02$ . The heavy dashed curve represents the underlying, reddened continuum model [ $M = 1.6 \times 10^{10} M_{\odot}$ ,  $\dot{M} = 4 M_{\odot} \text{ yr}^{-1}$ , and  $\cos i = 0.4$ ], while the heavy solid curve shows this model with emission and absorption lines as determined by the fits in KDZL. Some of the more prominent emission lines associated with the quasar are marked, and the large vertical line at  $\lambda_{\text{obs}} = 1056 \text{ \AA}$  shows the position of the hydrogen Lyman limit in the rest frame of the quasar. Earth symbols indicate wavelength regions that we have excluded from our fits because of the presence of geocoronal emission lines. Short vertical lines denote our chosen continuum points.

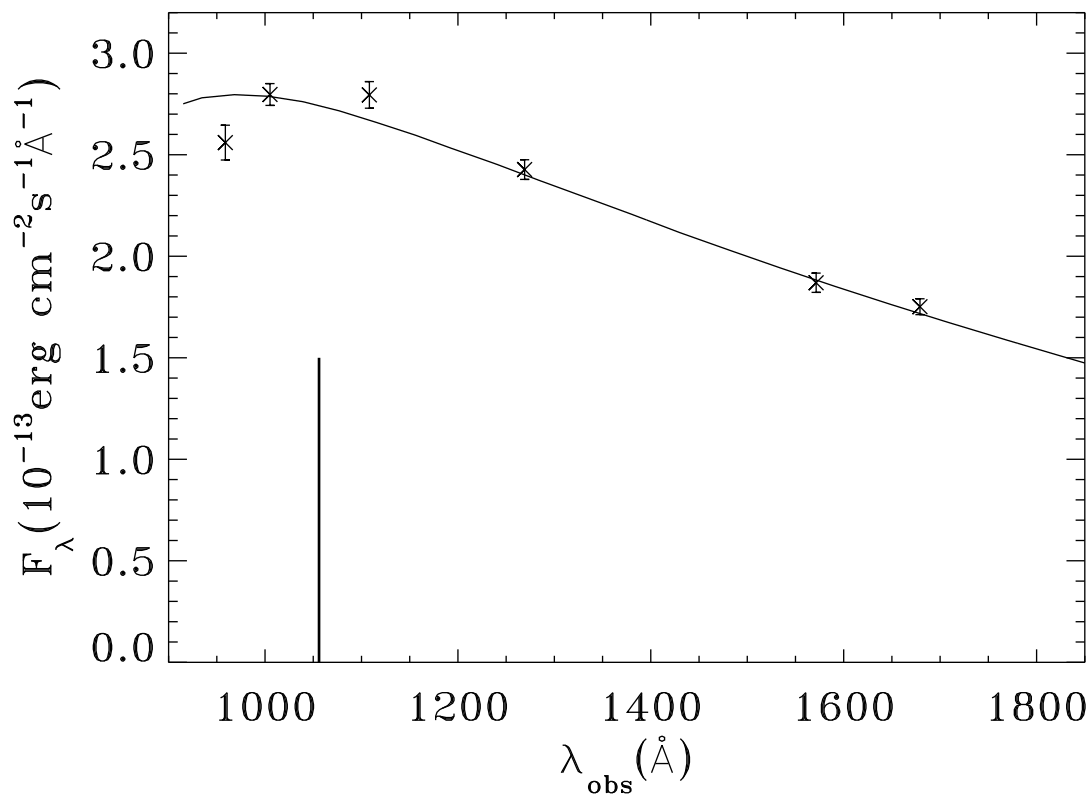


Fig. 2.— Best fit non-LTE Kerr disk continuum model to our six chosen continuum points of the December 1990 *HUT* data. The large vertical line again shows the position of the hydrogen Lyman limit in the rest frame of the quasar. The model parameters are  $M = 1.6 \times 10^{10} M_{\odot}$ ,  $\dot{M} = 4 M_{\odot} \text{ yr}^{-1}$ ,  $\cos i = 0.4$ , and  $E(B - V) = 0.024$ .

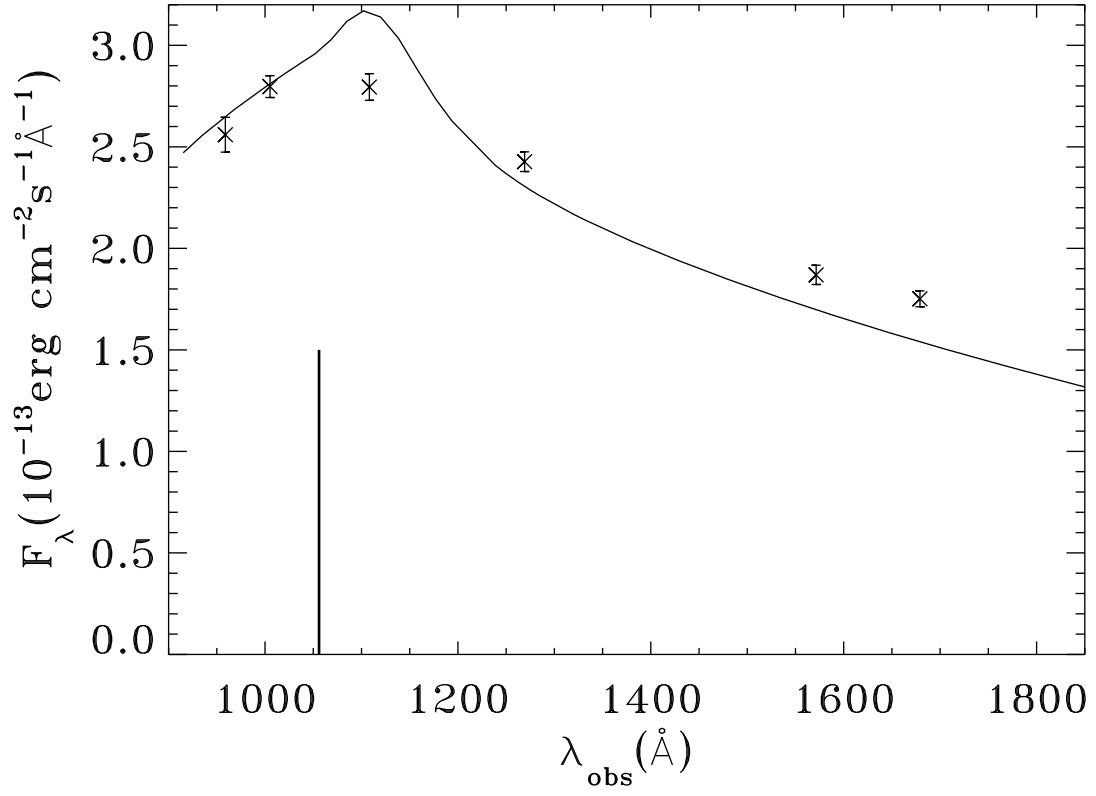
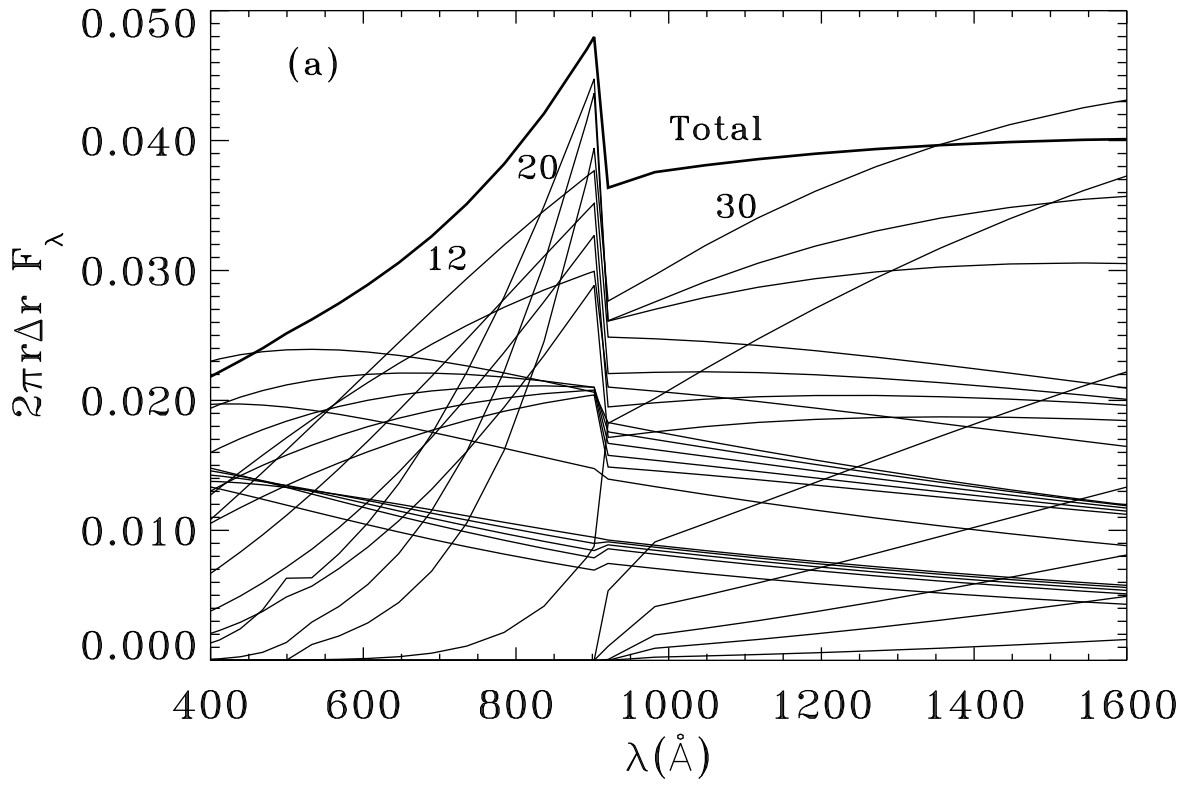


Fig. 3.— Same as figure 2, except showing the best fit non-LTE, near face-on ( $\cos i = 0.99$ ) Kerr disk continuum model. The model parameters are  $M = 2 \times 10^9 M_{\odot}$ ,  $\dot{M} = 4 M_{\odot} \text{ yr}^{-1}$ , and  $E(B - V) = 0.0253$ .



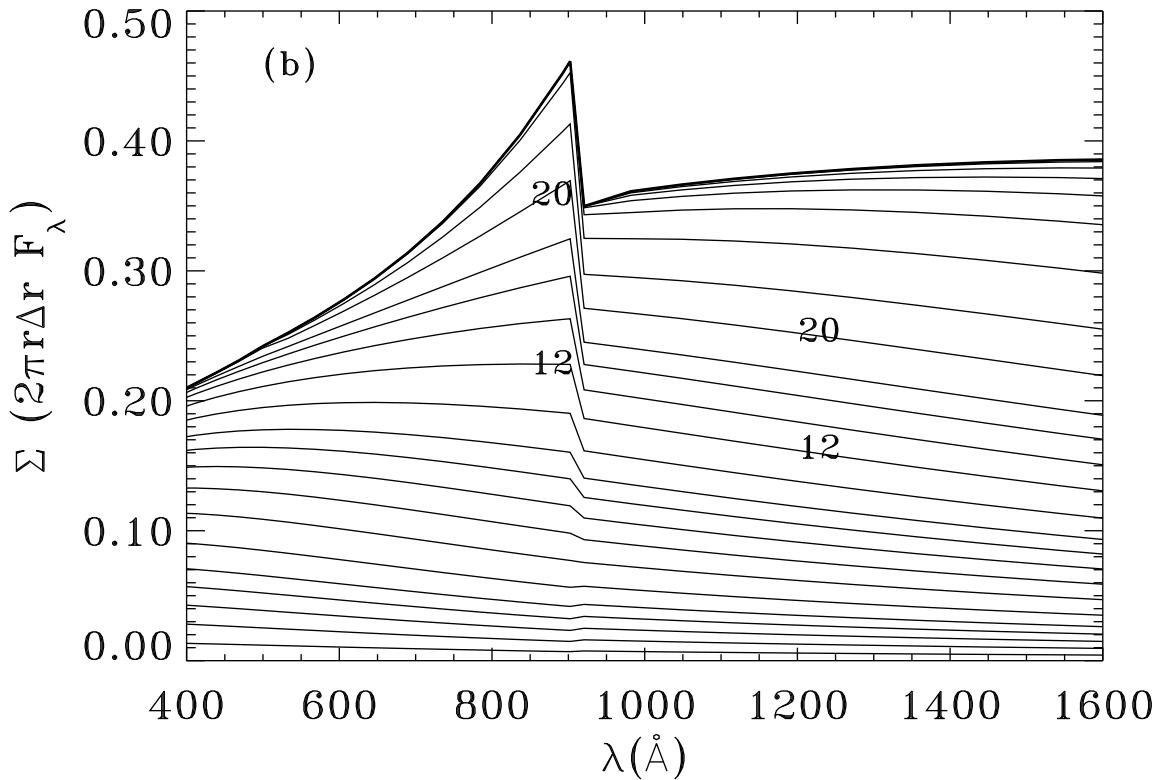


Fig. 4.— (a) Local emergent fluxes (in arbitrary units) from the various annuli contributing to the Kerr disk continuum model in figure 3. The flux from each annulus is multiplied by its nominal (Newtonian) surface area  $2\pi r \Delta r$  in order to weight its contribution to the total flux. The annuli contributing most to the flux around the Lyman limit are labeled with their radii in units of the gravitational radius  $GM/c^2$ . The curve labeled “Total” is the average flux from all the annuli, multiplied by 2.6 for clarity. (b) Cumulative sum of the local emergent fluxes. From bottom to top, the curves represent the contributions of all annuli out to radius 1.5, 2, 2.5, 3, 3.5, 4, 5, 6, 7, 8, 9, 10, 12, 14, 16, 18, 20, 25, 30, 40, 50, 60, 70, 80, and 90; in units of the gravitational radius. The topmost bold curve is the sum. Convergence is obtained in the Lyman continuum at about 30 gravitational radii, with annuli around 12 and 20 gravitational radii providing the dominant contribution. The cumulative sums out to these two annuli are labeled in the figure.

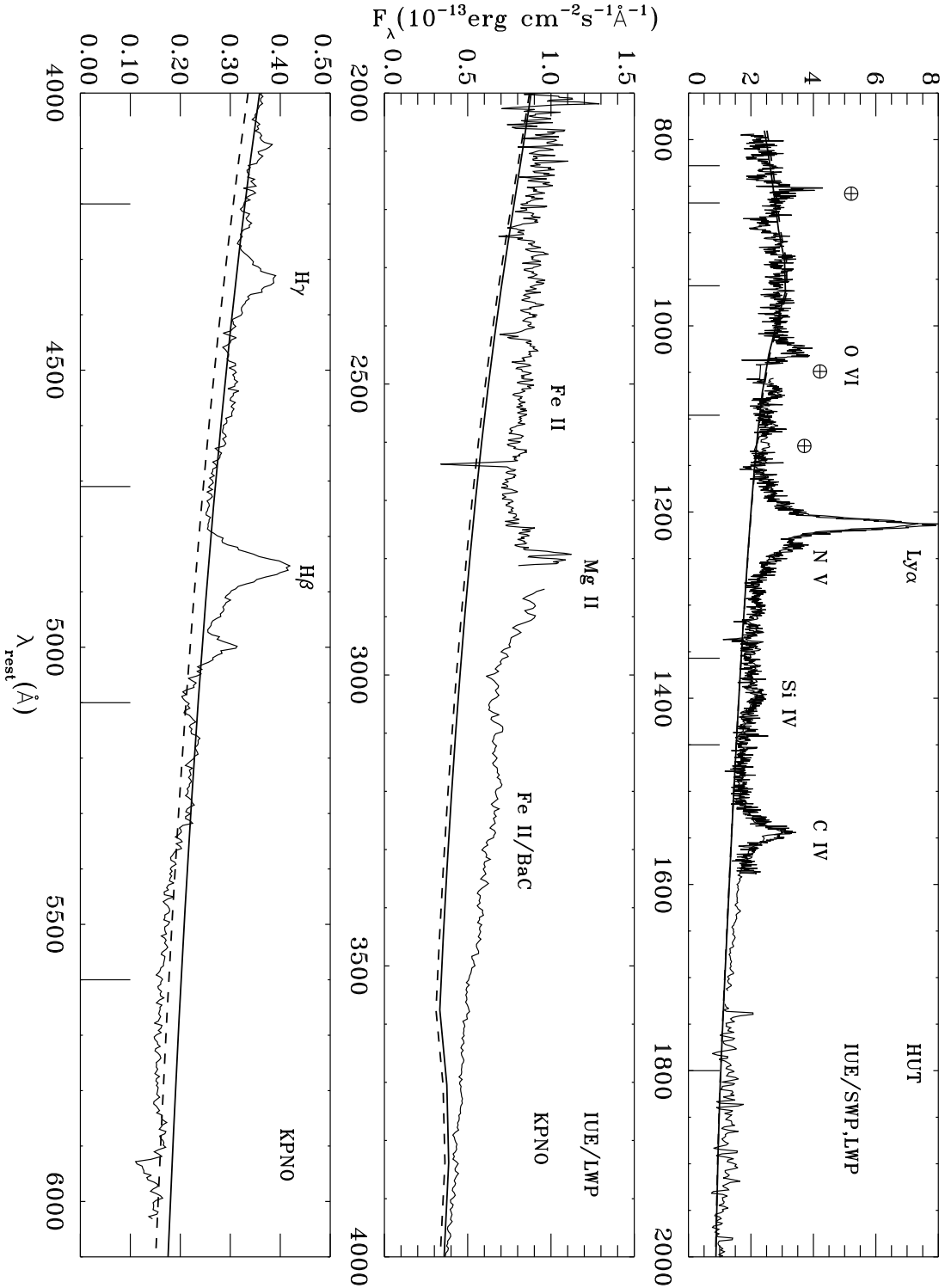


Fig. 5.— Best fit near face-on ( $\cos i = 0.99$ ) non-LTE Kerr models to the December 1990 3C 273 multiwavelength data (noisy curves). The smooth curves represent the underlying, reddened continuum models including (solid) and without (dashed) a possible blazar contribution (see text for details). Prominent emission lines associated with the quasar have been marked and the various observatories used to acquire data are indicated. Large vertical tick marks in the top and bottom figures indicate the locations of the eleven continuum points used in the fits.

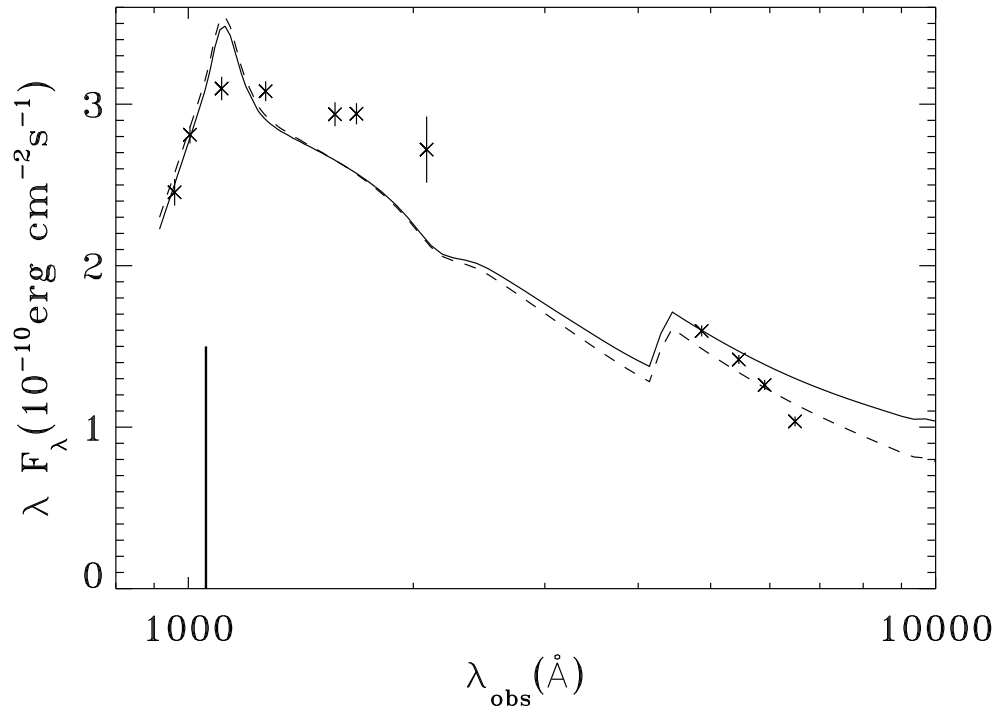


Fig. 6.— The same models as shown in figure 5, plotted against the eleven chosen continuum data points used in the fits. The vertical line shows the position of the hydrogen Lyman limit in the rest frame of the quasar. The dip in the model spectrum near 2000 Å is due to the 2200 Å feature in the reddening curve.

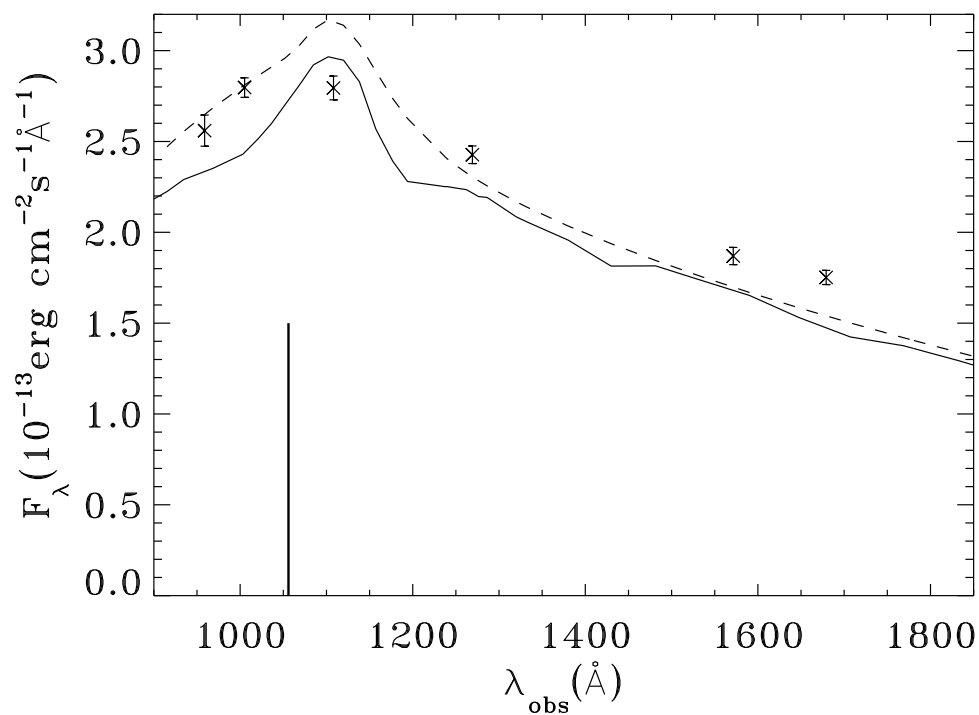


Fig. 7.— Same as figure 3, except showing a non-LTE, near face-on ( $\cos i = 0.99$ ) Kerr disk continuum model, including the effects of line blanketing (solid line). The model parameters are  $M = 2 \times 10^9 M_\odot$ ,  $\dot{M} = 4 M_\odot \text{ yr}^{-1}$ , and  $E(B - V) = 0.0253$ . The original model of figure 3 without line-blanketing, is shown as the dashed line.

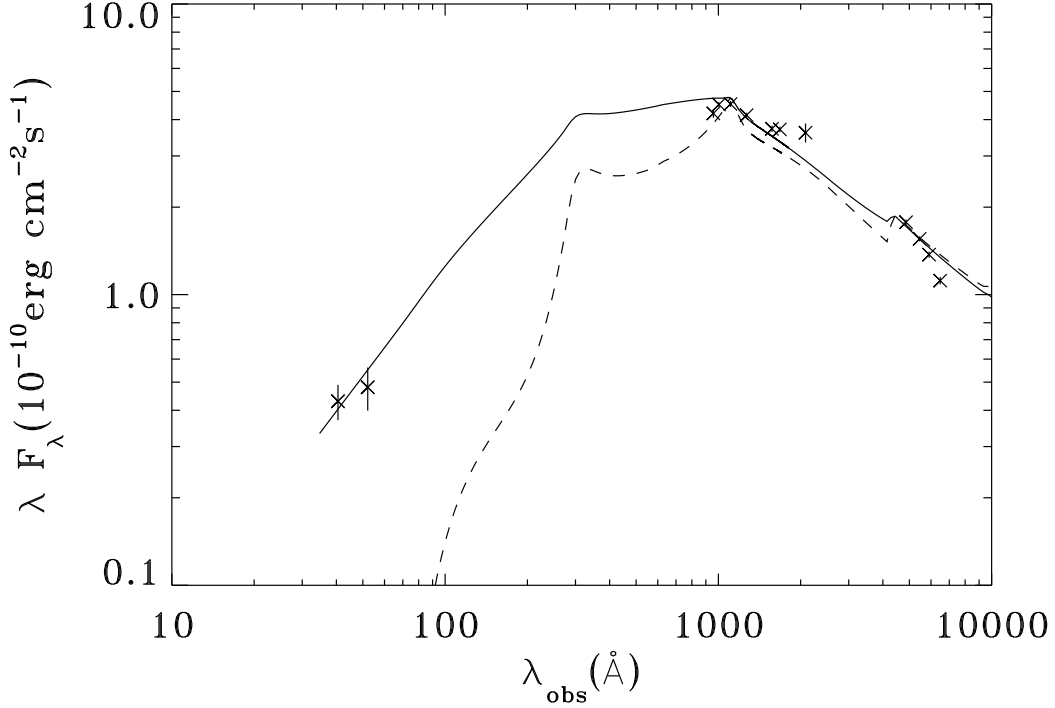


Fig. 8.— The energy distribution of 3C 273 from optical to X-rays during the December 1990 observing epoch. The two shortest wavelength data points were measured by *ROSAT*, while the longer wavelength points are the eleven optical/ultraviolet continuum data points used in our spectral fits. In contrast to all other plots in this paper, the data points here have been corrected for Galactic hydrogen absorption (in X-rays) and reddening (in the optical and ultraviolet) with  $E(B - V) = 0.032$ . The dashed curve shows our best fit Kerr model from figure 3, with  $M = 2 \times 10^9 M_{\odot}$ ,  $\dot{M} = 4 M_{\odot} \text{ yr}^{-1}$ , and  $\cos i = 0.99$ . The solid curve shows a Comptonized version of this model designed to go through the *ROSAT* data points. The Comptonizing medium for this model had a Thomson depth of unity and an electron temperature of  $3.3 \times 10^8 \text{ K}$ .

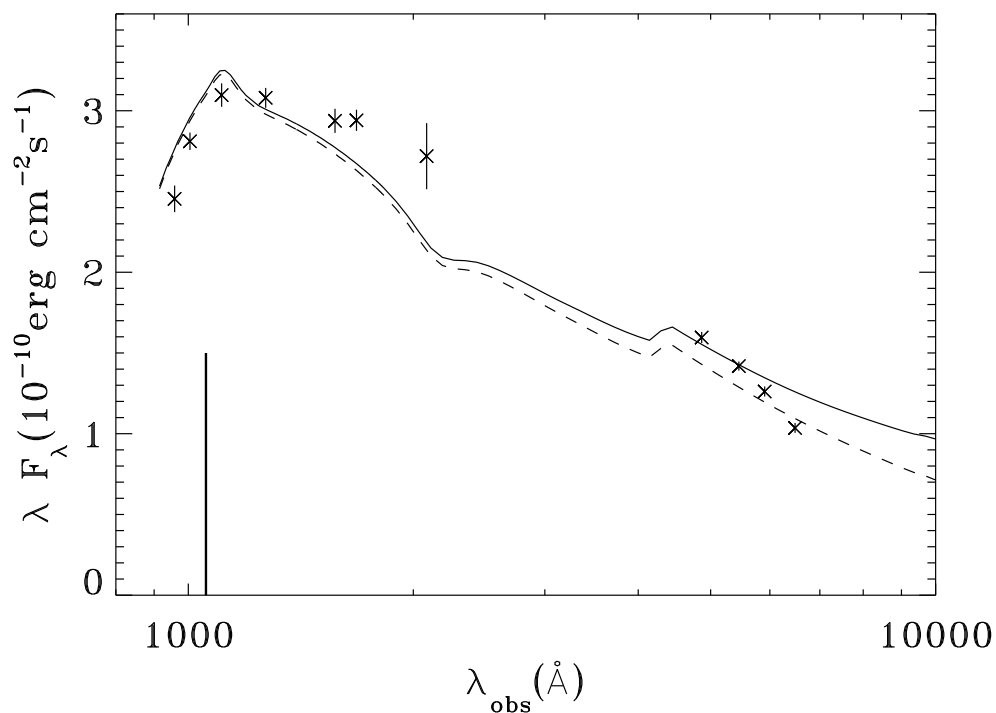


Fig. 9.— Same as figure 6 except for our Comptonized near face-on Kerr models. The model parameters are  $M = 2 \times 10^9 M_\odot$ ,  $\dot{M} = 4 M_\odot \text{ yr}^{-1}$ ,  $\cos i = 0.99$ , and  $E(B - V) = 0.032$ . The Comptonizing medium had a Thomson depth of unity and an electron temperature of  $3.3 \times 10^8 \text{ K}$ . The solid curve has an additional blazar component, while the dashed curve does not have such a component.

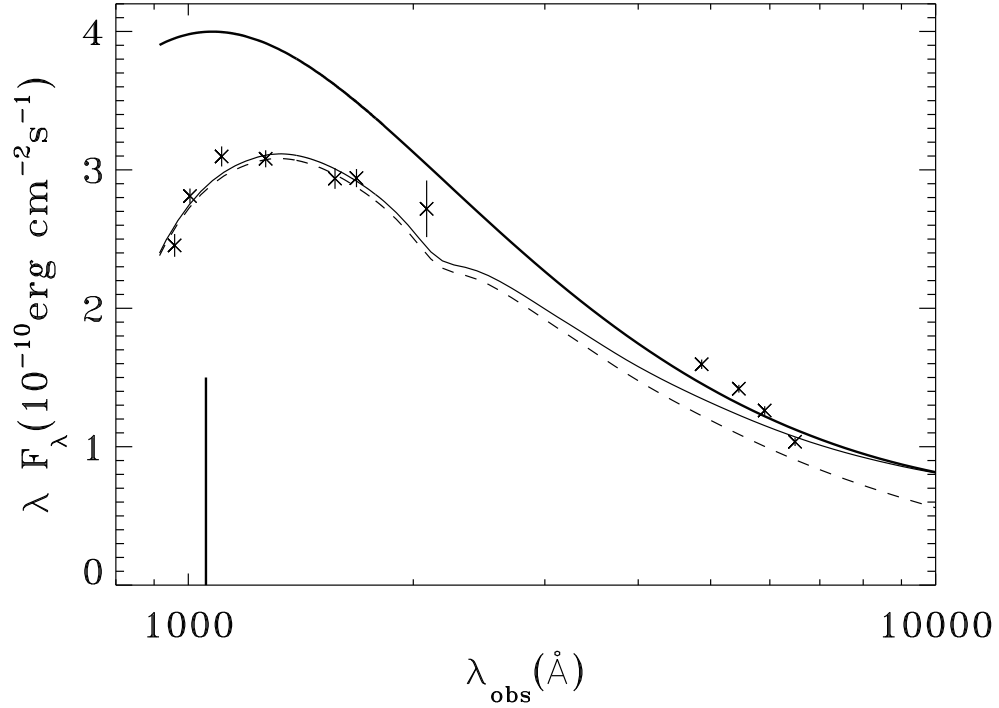


Fig. 10.— A multitemperature blackbody, near face-on ( $\cos i = 0.99$ ) disk model which provides a reasonable fit to the far ultraviolet data of 3C 723. The upper thick solid curve shows the model without reddening (but with a blazar component), while the lower curves show the reddened model with (solid) and without (dashed) a blazar component. The model parameters are  $a/M = 0.7$ ,  $M = 7 \times 10^8 M_\odot$ ,  $\dot{M} = 6.8 M_\odot \text{ yr}^{-1}$ , and a Galactic reddening of  $E(B - V) = 0.025$ .